

Optical properties of quasi-type-II structure in GaAs/GaAsSb/GaAs coaxial single quantum-well nanowires

Haolin Li,¹ Jilong Tang,^{1,a)} Yubin Kang,¹ Haixia Zhao,¹ Dan Fang,¹ Xuan Fang,¹ Rui Chen,^{2,b)} and Zhipeng Wei¹

¹State Key Laboratory of High Power Semiconductor Laser, School of Science, Changchun University of Science and Technology, 7089 Wei-Xing Road, Changchun 130022, People's Republic of China

²Department of Electrical and Electronic Engineering, Southern University of Science and Technology, Shenzhen, Guangdong 518055, People's Republic of China

(Received 27 August 2018; accepted 19 November 2018; published online 6 December 2018)

The GaAsSb-based quantum well plays a very important role in optoelectronic devices due to its excellent wavelength tunability. When the dimension reduces, the quantum confinement effect will take place and the quantum well in nanowires will show many interesting characteristics. GaAsSb-based quantum-well nanowires are of contemporary interest. However, the properties of the quasi-type-II structure in a single quantum well nanowire have been rarely investigated. Here, we grow GaAs/GaAs_{0.92}Sb_{0.08}/GaAs coaxial single quantum-well nanowires and discussed their power-dependent and temperature-dependent photoluminescence. We find that due to the small band offset of conduction bands, both type-I like and type-II like emission exist in our nanowires. When electrons obtain enough thermal energy through collisions or surrounding environment, they will overcome the barrier and diffuse to the GaAs conduction band, which contributes to the type-II like recombination. These results show the optical property of the quasi-type-II quantum well in nanowires, which can pave the way toward future nanoscale quantum well devices. *Published by AIP Publishing.*

<https://doi.org/10.1063/1.5053844>

As one of the most important narrow-band ternary alloys, GaAsSb is an attractive material for the fabrication of optoelectronic devices with high tunability that can cover a wide infrared wavelength range (from 870 to 1720 nm at room temperature) by adjusting the Sb content.¹ Due to the suitable energy band structure, they can form quantum wells (QWs) with other semiconductors like GaAs,² and AlGaAs;^{3,4} this architecture would be highly suitable for optoelectronic applications such as light-emitting diodes,^{5,6} lasers,^{2,7} and ultrafast photodetectors.⁸ When the dimension reduces, the quantum confinement effect will be more pronounced. Moreover, thanks to their atomically smooth walls, nanowires are naturally 1D optical waveguides, along which photons are allowed to propagate with low losses.⁹ Furthermore, semiconductor nanowires with high optical gain offer promising solutions for lasers with small footprints and low power consumption. Since Yang *et al.*¹⁰ first demonstrated the ZnO nanowire laser, people realized that it is feasible to obtain the laser in the nanowire. Various nanowire laser materials have sprung up like GaAs,¹¹ GaSb,¹² GaN,¹³ etc. However, lasing from GaAsSb-based nanowires has rarely been achieved. And, therefore, it is important to investigate the optical properties of GaAsSb-based nanostructures.

Several methods commonly used for the growth of nanostructures are hydrothermal methods,¹⁴ metal organic chemical vapor deposition (MOCVD),¹¹ and molecular beam epitaxy (MBE),^{1,15} As a traditional growth method, the hydrothermal method has simple operation and low cost, but it cannot accurately regulate the growth of materials. Moreover, impurity will be easily introduced due to non-vacuum

conduction. Both MOCVD and MBE can perform nanostructure growth at the atomic level. Due to the physical growth method and ultra-high vacuum, MBE can control the composition of each material more precisely compared to MOCVD.

The band structure of the GaAs/GaAsSb heterojunction is critical for device application. For ternary alloys, the bandgap of the material will be influenced by the composition, and the band structure of the heterojunction is affected by the band alignment of the materials. As pointed out by researchers,¹⁶ the GaAs/GaAsSb quantum well can form a type-I band alignment at the lower Sb mole fractions and a type-II band alignment when the Sb composition is high.

In this work, we use MBE to precisely control the nanowire components and grow GaAs/GaAs_{1-x}Sb_x/GaAs coaxial single quantum-well nanowires. The optical properties of high-quality GaAs/GaAsSb/GaAs coaxial single quantum well nanowires were investigated by photoluminescence (PL) spectroscopy at various excitation intensities and temperatures. From these spectra, the excitonic transitions can be clearly identified. It is shown that a quasi-type-II quantum well structure¹⁷ exists with a type-I like alignment and a small conduction band offset. In this structure, both type-I like and type-II like behaviors exist. With the temperature increase, some of the trapped electrons gain enough energy and contribute to type-II like emission. Through analyzing the results, the dynamics of the quasi-type-II QWs in nanowires is understood which will be routinely used in different applications for nanoscale quantum well devices.

The GaAs/GaAs_{0.92}Sb_{0.08}/GaAs coaxial single quantum-well nanowires discussed in this work were grown by the Ga-assisted self-catalyzed method on a Si (111) substrate. The growth was performed using a DCA P600 solid source MBE system. Before being loaded into the MBE chamber,

^{a)}Electronic mail: j_l_tangcust@163.com

^{b)}Electronic mail: chen.r@sustc.edu.cn

the substrate was dealt with ultrasonic cleaning in ethanol solution for 5 min and then etched with hydrochloric acid. During the growth progress, As_4 and Sb_2 were used as the precursors. First, Ga droplets were deposited on the Si substrates with a beam equivalent pressure of Ga of 6.7×10^{-8} Torr. The GaAs core was grown with the Ga beam equivalent pressure kept at 6.7×10^{-8} Torr and the As beam equivalent pressure has been set to be 2.3×10^{-6} Torr, respectively. The V/III flux ratio was set as 34.3. After the GaAs core growth of 30 min, the beam equivalent pressure of As was reduced to 2.1×10^{-6} Torr, while the beam equivalent pressure of Ga maintains the same. At the same time, the Sb flux was turned on and the beam equivalent pressure of Sb was set to 1.9×10^{-7} Torr. After the 10 min GaAsSb shell growth, the Sb flux was turned off, and the beam equivalent pressure of As was turned back to 2.3×10^{-6} Torr. The GaAs cap layer was grown for 10 min. During the whole growth progress, the temperature was set to 600°C .

The morphological properties of nanowires were characterized by scanning electron microscopy (SEM, Hitachi S-4800) and high-angle annular dark field scanning transmission electron microscopy (HAADF-STEM, FEI Talos F200X) with energy-dispersive X-ray spectroscopy (EDX, EDAX). Optical properties of GaAs/GaAsSb/GaAs coaxial single quantum well nanowires were investigated by laser spectroscopy. A 655 nm semiconductor diode laser was used as the excitation source. The spot size of the laser beam was about 0.4 cm^2 . The emission was dispersed by HORIBA iHR550, and the PL signal was detected by an InGaAs detector. A standard phase lock-in amplifier technique was employed to improve the signal-to-noise ratio. The excitation power of the laser was fixed at 100 mW during the temperature-dependent PL measurement, and the temperature change within a helium closed-cycle cryostat. During the power-dependent PL measurement, the temperature of the sample was fixed at 10 K.

Structure characterization of the nanowires is shown in Fig. 1. From the SEM image, it can be seen that the nanowires are grown on the Si substrate with the length about $5\ \mu\text{m}$, while the diameter is around 200 nm. To better understand the structure of the nanowires, HAADF-STEM and EDX were used to confirm the sandwich structure and the component of Sb. In order to characterize the cross-section of the nanowires during the TEM measurement, we used the ultra-thin slicing method (distributing the nanowires in the resin and then slicing the sample). We have observed three

different samples, and both of them show similar information, which can be seen from Figs. 1(c) and 1(d). The core-shell structure exists and the thickness of the GaAsSb shell is about 10 nm. It is evident from the EDX spectrum (taken from a slanted section) that there is a slight inhomogeneity of Sb distribution and the average of the Sb component in the sample is about 8%.

With low concentration of Sb, the quantum well possesses a type-I like band structure.^{18,19} The bandgap of GaAs at room temperature is about 1.43 eV, while the bandgap of $\text{GaAs}_{1-x}\text{Sb}_x$ in the quantum well can be described by the empirical model proposed by Teissier *et al.*²⁰

$$E_g = 1.43 - 2.24x_{sb} + 1.97x_{sb}^2 \text{ (eV)}. \quad (1)$$

And the valence band discontinuity is given by

$$\Delta E_v(x_{sb}) = 1.97x_{sb} - 1.69x_{sb}^2 \text{ (eV)}. \quad (2)$$

In our work, it can be calculated that the bandgap of GaAsSb is about 1.26 eV and the conduction band offset is about 20 meV at 300 K, which is in good agreement with the result by Johnson *et al.*¹⁹ Inside the quantum well, the ground state energy will be slightly higher than the GaAsSb conduction band minimum. The conduction band offset is too small to effectively confine electrons inside the quantum wells. In contrast, the valence band offset is about 150 meV, and it is large enough to confine holes. Due to the small barrier, the wavefunction of electrons will extend to the conduction band of the GaAs barrier. And the GaAsSb well cannot effectively confine the electrons. When electrons obtain enough thermal energy through collisions or surrounding environment, they will have a greater chance to overcome the barrier and diffuse to the GaAs. The inhomogeneity of the Sb content observed in EDX mapping would also result in more type-I and type-II like band alignment along the tangential direction, which further supports the analysis. In other words, a quasi-type-II band structure exists in the coaxial single quantum-well nanowire.

Figure 2 plots the PL spectrum at low temperature (10 K). It is found that the shape of the emission is asymmetry and a long tail located in the low energy region can be observed. Therefore, there must be more than one type of emission mechanism involved. Three gauss peaks labeled as P1, P2, and P3 (from higher energy to lower energy) were used to fit this emission which completely coincides with the experimental results. The dotted line is the experimental data

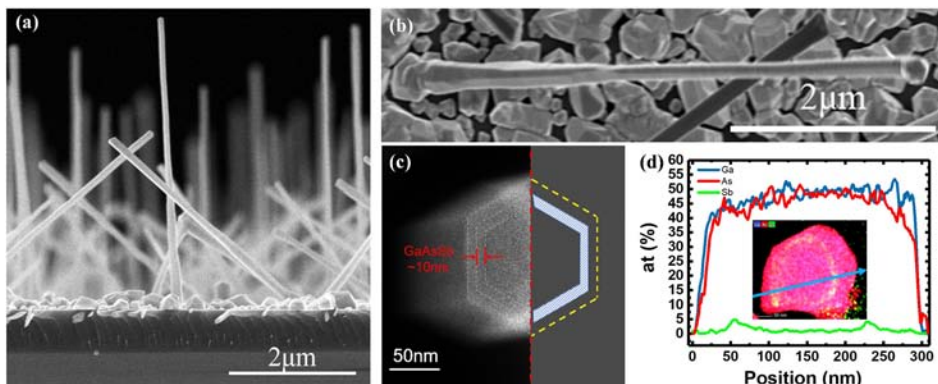


FIG. 1. (a) and (b) SEM image of GaAs/GaAsSb/GaAs coaxial single quantum-well nanowires. (c) HAADF-STEM image and schematic diagram of the core-shell structure. (d) EDX spectrum of the cross section.

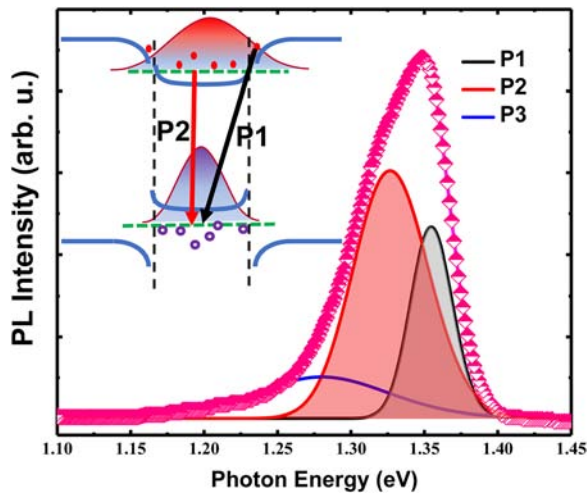


FIG. 2. Low temperature PL emission of GaAs/GaAsSb/GaAs coaxial single quantum-well nanowires, which is well fitted by Gaussian peaks (the solid line represents the fitting curve, and the dotted line is the experimental data).

and the solid colored line is the fitting result of three gauss peaks. The solid pink line indicates the integration of the individual fitted peaks. As discussed above, due to the small band offset between GaAs and GaAs_{0.92}Sb_{0.08}, electronics cannot be effectively confined in the quantum well. Therefore, it is supposed that at the high energy side, the emission of P1 (1.354 eV) may come from type-II like behavior transition that electrons from the GaAs barrier recombined with holes in the GaAsSb well. The dominated P2 peak (1.328 eV) represents a type-I like behavior transition that both electrons and holes are confined inside the well. Inhomogeneity of the Sb content in quantum wells can be used to explain the formation of the band tail of P3. The photon energy of P1, P2, and P3 is smaller than that of GaAs (which is 1.515 eV at 10 K); this indicates that the luminescence comes from the GaAsSb quantum well.

To further confirm the origin of the two peaks P1 and P2, power dependent PL measurement at low temperature (10 K) was carried out. The PL spectra of GaAs/GaAs_{0.92}Sb_{0.08}/GaAs nanowires under different excitation powers (1–100 mW) at 10 K are shown in Fig. 3(a). P1 and P2 can be clearly observed in all emissions. With the increase in excitation power, the intensity of P1 increases faster than that of P2, as it is shown in the inset of Fig. 3(a), the proportion of the two peaks has changed with excitation power. Furthermore, a gradual blue shift in the PL peak emission with increasing excitation power can be noted. Those phenomena can be described by the quasi-type-II band alignment. In this model, the conduction band offset between GaAs and GaAsSb is very small. Therefore, the wave-function of the electron will extend to the barrier layer. In contrast, the holes can be completely confined inside the well. Uneven distribution of electrons and holes will cause band bending, where electrons will be localized near the interface and recombine with the hole in the GaAsSb well. With the increase in excitation power, more electrons will jump to the GaAs barrier and lead to the increase in the band bending degree, as shown in Fig. 3(b). Due to the band bending effect, those electrons will occupy higher energy positions, which results in the blue shift of the emission and the intensity proportion change.

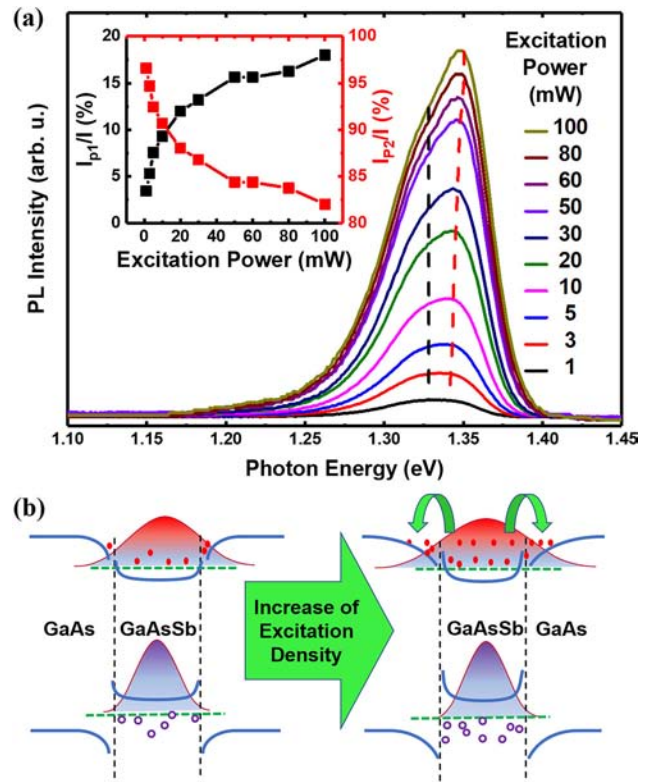


FIG. 3. (a) Low temperature photoluminescence spectra of GaAs/GaAsSb/GaAs NWs under different excitation intensities. The inset shows that the proportion of P1 will increase rapidly with increasing excitation power; (b) Schematic band structure of the GaAs/GaAsSb/GaAs nanowire with low and high excitation densities.

Figure 4 plots the temperature dependent PL emission under an excitation power of 100 mW. The peak P2 exists at temperatures from 10 to 180 K, while disappearing when the temperature is above 200 K. It is noted from Fig. 4 that the intensity of P2 decreases significantly with temperature above 100 K. In contrast, peak P1 exists for the whole temperature range from 10 to 240 K and dominates the emission. At high temperature than 200 K, the shape of the P1 emission changes to be symmetric. With the temperature increase, the electrons confined in quantum well gain enough thermal energy and transitioned to the barrier, which contributes to the type-II like emission.

To further study the characteristics of P1 and P2 from the shallow quantum wells, the peak emission energy of the sample as a function of temperature is plotted in Fig. 4(b). The temperature dependence of semiconductor bandgap shrinkage can be well described by the Varshni^{21,22} model, expressed as

$$E_g(T) = E_g(0) - \frac{\alpha T^2}{T + \beta}, \quad (3)$$

where $E_g(0)$ is the bandgap at 0 K, α is the temperature coefficient, and β is a parameter related to the Debye temperature. For P1, $E_g(0) = 1.354$ eV, $\alpha = 6.44 \times 10^{-4}$ eV/K, $\beta = 345 \pm 40$ K, For P2, $E_g(0) = 1.327$ eV, $\alpha = 5.11 \times 10^{-4}$ eV/K, $\beta = 166 \pm 24$ K. The obtained parameters are close to those of GaAs bulk and nanowires.^{22,23}

Figure 4(c) shows the normalized integrated PL intensity of P1 and P2 at different temperatures. As have pointed

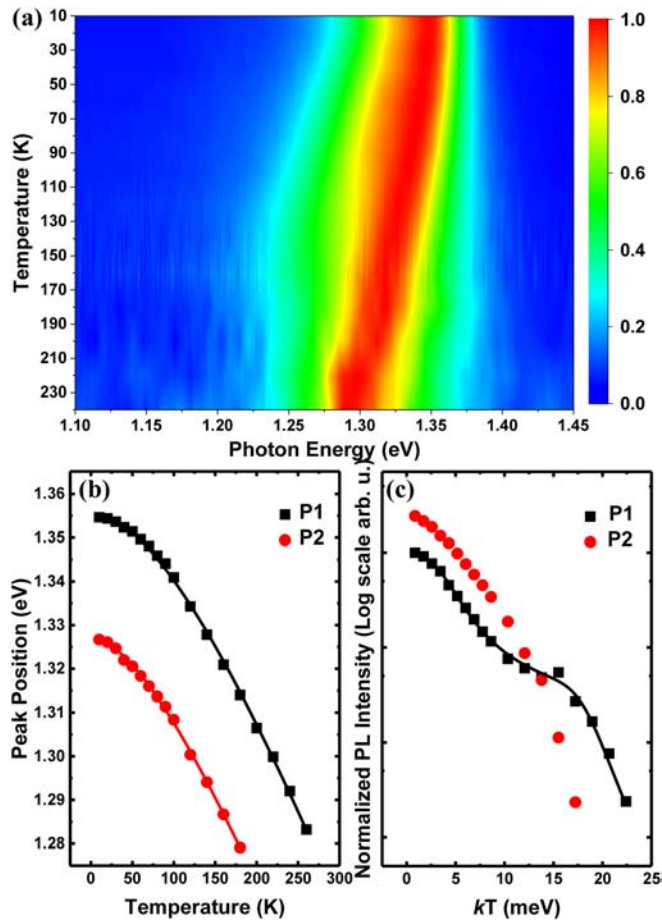


FIG. 4. (a) Normalized temperature dependent PL curve from 10 to 240 K. (b) Peak position red shift with temperature which is well fitted with the Varshni equation. (c) The integrated PL intensity (normalized) of the samples with temperatures.

out, the peak P2 dominates at the low temperature (10–100 K), when the temperature increases up to 100 K, the intensity of P2 peak drops sharply until disappearing. In contrast, P1 exists for the whole temperature range and drops slowly at temperatures from 100 to 180 K. This is because the carriers in the quantum well get enough thermal energy to overcome the barrier to GaAs conduction band, which contributes to the type-II like emission.

To discuss the thermal activation of carriers, the model proposed by Popescu *et al.*^{24,25} was used to describe the temperature dependent PL intensity. The integrated PL intensity could be expressed as

$$\frac{R_r N_D}{G_e} = \left\{ 1 + \frac{K_0}{1 + \exp\left(-\frac{E_b}{kT}\right)} \left[1 + \sum_{i=1}^2 K_i \exp\left(-\frac{E_i}{kT}\right) \right] \right\}^{-1} \quad (4)$$

($i = 1$ or 2),

where R_r is the electron-hole pair recombination rate, and N_D is the population of electrons. G_e is the number of carriers captured by the QW per unit time. K_0 is a constant, k is the Boltzmann constant, T represents temperature, and E_b shows the potential of the barrier. With temperature increase, thermal escaped carriers should be considered, where i is the number of thermal escape channels for carriers, K_i is a

constant, and E_i represents the thermal activation energy. By fitting the experimental data of P1, the temperature dependence of QW integrated PL intensity could be perfectly fitted when two thermal escape channels are considered. The value of the potential barrier of E_b is estimated to be 6.2 meV, and the 18 meV and 305 meV activation energy could be considered for the thermal activated nonradiative defects. It is noted that the value calculated above is smaller than the conduction band offset between GaAs and GaAsSb. This is because in the quantum well, the ground state energy will be slightly higher than the GaAsSb conduction band minimum. We calculated the Schrödinger equation for a finite deep square quantum well (with depth of 20 meV and width of 10 nm), and found that the ground state is ~ 12 meV above the conduction band minimum, then the potential barrier that the electrons should overcome is 6–8 meV. This value is basically consistent with the results we obtained from fitting.

In summary, we have investigated the optical properties of GaAs/GaAs_{0.92}Sb_{0.08}/GaAs coaxial single quantum well nanowires grown by MBE. It was found that a quasi-type-II band alignment formed at the lower Sb molar fractions, in which a type-I like structure exists with a small conduction band offset. The offset of the conduction band is too small to fully confine carriers, and therefore, both type-I like and type-II like behaviors exist. When electrons obtain enough thermal energy through collisions or surrounding environment, they will overcome the barrier and diffuse to the GaAs conduction band, and finally the type-II like recombination dominates. This work shows the dynamics of GaAs/GaAsSb quantum well nanowires with a quasi-type-II band structure, which may be used in different applications, and benefits the research of nanoscale quantum well devices.

This work was supported by the National Natural Science Foundation of China (Nos. 61474010, 61574022, 61504012, 61674021, 61704011, 11404219, 11574130, and 11674038), the Foundation of State Key Laboratory of High Power Semiconductor Lasers, the Developing Project of Science and Technology of Jilin Province (Nos. 20160519007JH, 20160520117JH, 20170520118JH, 20160101255JC, 20160204074GX, and 20170520117JH), and the Foundation of NANO X (No. 18JG01). R.C. acknowledges the national 1000 plan for young talents and Shenzhen Science and Technology Innovation Commission (Projects Nos. KQJSCX20170726145748, JCYJ20150930160634263, and KQTD2015071710313656).

¹L. Li, D. Pan, Y. Xue, X. Wang, M. Lin, D. Su, Q. Zhang, X. Yu, H. So, D. Wei, B. Sun, P. Tan, A. Pan, and J. Zhao, *Nano Lett.* **17**(2), 622–630 (2017).

²D. Ren, L. Ahtapodov, J. S. Nilsen, J. Yang, A. Gustafsson, J. Huh, G. J. Conibeer, A. T. J. van Helvoort, B. O. Fimland, and H. Weman, *Nano Lett.* **18**(4), 2304–2310 (2018).

³X. Yuan, D. Saxena, P. Caroff, F. Wang, M. Lockrey, S. Mokkapatil, H. H. Tan, and C. Jagadish, *J. Phys. Chem. C* **121**(15), 8636–8644 (2017).

⁴X. Ge, D. Wang, X. Gao, X. Fang, S. Niu, H. Gao, J. Tang, X. Wang, Z. Wei, and R. Chen, *Phys. Status Solidi RRL* **11**(3), 1700001 (2017).

⁵K. Tomioka, J. Motohisa, S. Hara, K. Hiruma, and T. Fukui, *Nano Lett.* **10**(5), 1639–1644 (2010).

⁶F. Qian, S. Gradecak, Y. Li, W. C. Wen, and C. M. Lieber, *Nano Lett.* **5**(11), 2287–2291 (2005).

⁷F. Qian, Y. Li, S. Gradecak, H. G. Park, Y. Dong, Y. Ding, Z. L. Wang, and C. M. Lieber, *Nat. Mater.* **7**(9), 701–706 (2008).

- ⁸N. Erhard, S. Zenger, S. Morkötter, D. Rudolph, M. Weiss, H. J. Krenner, H. Karl, G. Abstreiter, J. J. Finley, G. Koblmüller, and A. W. Holleitner, *Nano Lett.* **15**(10), 6869–6874 (2015).
- ⁹N. P. Dasgupta, J. Sun, C. Liu, S. Brittman, S. C. Andrews, J. Lim, H. Gao, R. Yan, and P. Yang, *Adv. Mater.* **26**(14), 2137–2184 (2014).
- ¹⁰M. H. Huang, S. Mao, H. Feick, H. Yan, Y. Wu, H. Kind, E. Weber, R. Russo, and P. Yang, *Science* **292**(5523), 1897–1899 (2001).
- ¹¹D. Saxena, S. Mokkalapati, P. Parkinson, N. Jiang, Q. Gao, H. H. Tan, and C. Jagadish, *Nat. Photonics* **7**(12), 963–968 (2013).
- ¹²A. H. Chin, S. Vaddiraju, A. V. Maslov, C. Z. Ning, M. K. Sunkara, and M. Meyyappan, *Appl. Phys. Lett.* **88**(16), 163115 (2006).
- ¹³C. Li, J. B. Wright, S. Liu, P. Lu, J. J. Figiel, B. Leung, W. W. Chow, I. Brener, D. D. Koleske, T. S. Luk, D. F. Feezell, S. R. Brueck, and G. T. Wang, *Nano Lett.* **17**(2), 1049–1055 (2017).
- ¹⁴X. Fang, Z. Wei, Y. Yang, R. Chen, Y. Li, J. Tang, D. Fang, H. Jia, D. Wang, J. Fan, X. Ma, B. Yao, and X. Wang, *ACS Appl. Mater. Interfaces* **8**(3), 1661–1666 (2016).
- ¹⁵Y. Zhang, J. Wu, M. Aagesen, J. Holm, S. Hatch, M. Tang, S. Huo, and H. Liu, *Nano Lett.* **14**(8), 4542–4547 (2014).
- ¹⁶S. V. Morozov, D. I. Kryzhkov, A. N. Yablonsky, A. V. Antonov, D. I. Kuritsin, D. M. Gaponova, Y. G. Sadofyev, N. Samal, V. I. Gavrilenko, and Z. F. Krasilnik, *J. Appl. Phys.* **113**(16), 163107 (2013).
- ¹⁷P. Maity, T. Debnath, and H. N. Ghosh, *J. Phys. Chem. C* **119**(46), 26202–26211 (2015).
- ¹⁸J. B. Wang, S. R. Johnson, S. A. Chaparro, D. Ding, Y. Cao, Y. G. Sadofyev, Y. H. Zhang, J. A. Gupta, and C. Z. Guo, *Phys. Rev. B* **70**(19), 195339 (2004).
- ¹⁹S. R. Johnson, C. Z. Guo, S. Chaparro, Y. G. Sadofyev, J. Wang, Y. Cao, N. Samal, J. Xu, S. Q. Yu, D. Ding, and Y. H. Zhang, *J. Cryst. Growth* **251**(1), 521–525 (2003).
- ²⁰R. Teissier, D. Sicault, J. C. Harmand, G. Ungaro, G. Le Roux, and L. Largeau, *J. Appl. Phys.* **89**(10), 5473–5477 (2001).
- ²¹Y. P. Varshni, *Physica* **34**(1), 149–154 (1967).
- ²²P. Lautenschlager, M. Garriga, S. Logothetidis, and M. Cardona, *Phys. Rev. B* **35**(17), 9174–9189 (1987).
- ²³A. M. Graham, P. Corfdir, M. Heiss, S. Conesa-Boj, E. Uccelli, A. Fontcuberta i Morral, and R. T. Phillips, *Phys. Rev. B* **87**(12), 125304 (2013).
- ²⁴D. Popescu, P. Eliseev, A. Stintz, and K. Malloy, *Semicond. Sci. Technol.* **19**(1), 33–38 (2003).
- ²⁵R. Chen, H. Y. Liu, and H. Sun, *J. Appl. Phys.* **107**(1), 013513 (2010).